AGU PUBLICATIONS

Geophysical Research Letters

RESEARCH LETTER
10.1002/2017GL075034

Key Points:
- Observational analysis reveals distinct evolution of atmospheric teleconnections and U.S. precipitation anomalies during multiyear La Niña
- La Niña teleconnections remain strong from the first to the second NH winter despite weakening of the equatorial Pacific cooling
- Large-scale atmospheric circulation appears more sensitive to broad tropical Pacific SST anomalies than those intensified at the equator

Supporting Information:
- Supporting Information S1

Correspondence to:
Y. M. Okumura,
yukoo@ig.utexas.edu

Citation:
Okumura, Y. M., DiNezio, P., & Deser, C. (2017). Evolving impacts of multiyear La Niña events on atmospheric circulation and U.S. drought. *Geophysical Research Letters, 44*, 11,614–11,623. https://doi.org/10.1002/2017GL075034

Received 21 JUL 2017
Accepted 13 OCT 2017
Accepted article online 20 OCT 2017
Published online 27 NOV 2017

Evolving Impacts of Multiyear La Niña Events on Atmospheric Circulation and U.S. Drought

Yuko M. Okumura[1], **Pedro DiNezio**[1], **and Clara Deser**[2]

[1]Institute for Geophysics, Jackson School of Geosciences, University of Texas at Austin, Austin, TX, USA, [2]Climate and Global Dynamics Laboratory, National Center for Atmospheric Research, Boulder, CO, USA

Abstract Wintertime precipitation over the southern U.S. is known to decrease with interannual cooling of the equatorial Pacific associated with La Niña, which often persists 2 years or longer. Composite analysis based on a suite of observational and reanalysis data sets covering the period 1901–2012 reveals distinct evolution of atmospheric teleconnections and U.S. precipitation anomalies during multiyear La Niña events. In particular, atmospheric circulation anomalies strengthen and become more zonally elongated over the North Pacific in the second winter compared to the first winter. U.S. precipitation deficits also remain large, while the region of reduced precipitation shifts northeastward in the second winter. This occurs despite a significant weakening of the equatorial Pacific cooling in the second winter and suggests that the large-scale atmospheric circulation is more sensitive to tropical sea surface temperature anomalies of broader meridional extent. Given the extended climatic impacts, accurate prediction of La Niña duration is crucial.

1. Introduction

The El Niño–Southern Oscillation (ENSO) phenomenon in the equatorial Pacific is the dominant mode of climate variability on interannual time scales (e.g., Chang et al., 2006; Neelin et al., 1998; Wallace et al., 1998; Wang & Picaut, 2004). Warm (El Niño) and cold (La Niña) phases of ENSO typically last 1–2 years and occur approximately every 3–8 years. Both El Niño and La Niña exhibit strong seasonality and tend to develop in late boreal spring/summer, peaking toward the end of the calendar year. El Niño and La Niña, however, are not a simple mirror image and exhibit asymmetry in their spatial pattern and seasonal evolution, especially for strong events, because of nonlinearities in the tropical ocean-atmosphere system (e.g., Burgers & Stephenson, 1999; DiNezio & Deser, 2014; Dommenget et al., 2013; Hoerling et al., 1997; Hu et al., 2014; Kang & Kug, 2002; Kessler, 2002; McGregor et al., 2013; McPhaden & Zhang, 2009; Ohba & Ueda, 2009; Okumura & Deser, 2010). In particular, El Niño events tend to decay rapidly after the mature phase, but many La Niña events persist through the following year and reintensify in the subsequent winter (Okumura & Deser, 2010).

The equatorial Pacific sea surface temperature (SST) cooling associated with La Niña has been linked to wintertime precipitation deficits over the southern U.S. (e.g., Dai et al., 1998; Kiladis & Diaz, 1989; Lau & Sheu, 1988; Mo & Schemm, 2008; Ropelewski & Halpert, 1989) (see Seager & Hoerling, 2014 and Schubert et al., 2016 for recent synthesis studies). The SST cooling suppresses atmospheric deep convection in the equatorial Pacific, and the related change in atmospheric heating forces a large-scale atmospheric Rossby wave into the Northern Hemisphere (NH), displacing the subtropical jet and storm track to the north over the Pacific and North America (e.g., Trenberth et al., 1998). The northward shift of storm track leads to a reduction in transient moisture flux convergence across the southern tier of the U.S. (Seager, Harnik, et al., 2005; Wang & Schubert, 2014). Previous studies of La Niña teleconnections, however, did not distinguish between single-year and multiyear events, and it is not clear how multiyear La Niña affects the evolution of atmospheric teleconnections and U.S. precipitation during the course of these events. It is crucial to understand the evolving impacts of multiyear La Niña events given their potential linkages to prolonged droughts and associated socioeconomic impacts (e.g., Cole et al., 2002; Hoerling & Kumar, 2003; Seager, Kushnir, et al., 2005).

The present study investigates the atmospheric teleconnections from the tropical Pacific during the first and second NH winters of multiyear La Niña events and their impacts on U.S. precipitation, using a suite of observational and reanalysis data sets covering the period 1901–2012. Atmospheric model experiments are also compared with the observational results. Section 2 describes the data and methods used in this study. Results from the observational analysis of multiyear La Niña events are reported in section 3. Section 4 summarizes the main results and discusses the outstanding issues for future investigation.

2. Data and Methods

In this study multiyear La Niña events are defined based on monthly SST anomalies averaged in the Niño-3.4 region (5°S–5°N, 120°–170°W; the Niño-3.4 index) from the Hadley Centre Sea Ice and SST (HadISST) data set (Rayner et al., 2003) for 1900–2016. The monthly Niño-3.4 index is linearly detrended and smoothed with a 3 month running mean filter prior to defining La Niña events. We denote the year when La Niña first develops as year 0 and the subsequent year as year 1. During multiyear La Niña events, equatorial SST cooling intensifies every boreal winter and peak cooling often weakens after the first winter. We identify a multiyear La Niña event when the Niño-3.4 index falls below −0.75 standard deviations in any month during October (0) to February (1) and remains below −0.5 standard deviations in any month during October (1) to February (2). (The standard deviation is calculated separately for each month.) Based on this criterion, we identify 10 multiyear La Niña events between 1900 and 2016 (1908, 1916, 1949, 1954, 1970, 1973, 1983, 1998, 2007, and 2010 as year 0). Figure S1 in the supporting information shows the Niño-3.4 index and the selection of multiyear La Niña events. About half of all La Niña events last longer than 2 years. Composite evolution of the Niño-3.4 index for multiyear La Niña events is presented in Figure S2.

We form seasonal composites of SST, precipitation, and atmospheric circulation anomalies for the 10 multiyear La Niña events, using SSTs from HadISST on a 1° grid, terrestrial precipitation from the Global Precipitation Climatology Centre (GPCC) version 7 on a 1.0° grid (Schneider et al., 2016), and sea level pressure (SLP), 200 hPa geopotential height (Z200) and zonal wind (U200), and precipitation from the Twentieth Century Reanalysis (20CR) version 2 on a 2° grid (Compo et al., 2011). Monthly anomalies of these variables are calculated for the common data period of 1901–2012 and linearly detrended prior to the analysis. It is noted that the results of composite analysis are not affected by decadal variability that is present in the detrended data. To reduce aliasing from subseasonal variability, the anomalies are averaged over extended NH cold (November–April) and warm (May–October) seasons. Statistical significance of the composite anomalies is evaluated through a two-tailed *t* test at the 90% confidence level. We also examine the robustness of the composites based on physical consistency between the different fields and whether the composites are replicated in different subsets and random samples of the events and in different data sets (National Centers for Environmental Prediction-National Center for Atmospheric Research (NCEP-NCAR) reanalysis (Kalnay et al., 1996) for 1948–2012 and the National Oceanic and Atmospheric Administration (NOAA) optimum interpolation SST (OISST) version 2 (Reynolds et al., 2002) and the European Centre for Medium-Range Weather Forecasts (ECMWF) interim reanalysis (ERA-Interim) (Dee et al., 2011) for 1982–2012). The observational analysis is also compared with atmospheric model simulations forced with observed SSTs (Hurrell et al., 2008; Huang et al., 2015) using the Community Atmosphere Model (CAM) versions 4 and 5 (Hurrell et al., 2013) and the Geophysical Fluid Dynamics Laboratory (GFDL) Atmosphere Model version 2.1 (AM2.1) (Li et al., 2010) (Text S1).

3. Results

Figure 1 shows composite anomalies of SST, SLP, terrestrial precipitation, and U200 for the first and second cold seasons of 10 multiyear La Niña events during 1901–2012. The main features of the teleconnection patterns are similar between the first and second cold seasons. In both years, SLP increases over the central North Pacific in association with the tropical Pacific SST cooling, weakening the wintertime Aleutian low. SST warming on the southern flank of this anomalous high pressure is consistent with inferred reduction in surface winds. Over the U.S., upper tropospheric zonal wind anomalies show a meridional dipole pattern, indicative of a weakening and northward shift of the subtropical westerly jet. In association with the weakened westerly winds in the upper troposphere, precipitation decreases across the southern tier of the U.S. These main features of cold season composite anomalies are statistically significant at the 90% confidence level in both the first and second years (Figures S3 and S4). During the warm season, on the other hand, U.S. precipitation anomalies are not as large and geographically coherent as those for the cold season (Figure S5) and the lack of statistical significance suggests limited predictability. Thus, we focus on the analysis of cold season anomalies in the rest of the paper.

The composite analysis of cold season anomalies reveals not only the similarities but also notable differences between the first and second years of multiyear La Niña events (Figure 1). First, the peak SST cooling in the central equatorial Pacific (150°W–180°) weakens by 28% (−1.25 to −0.90°C) from the first to the second cold

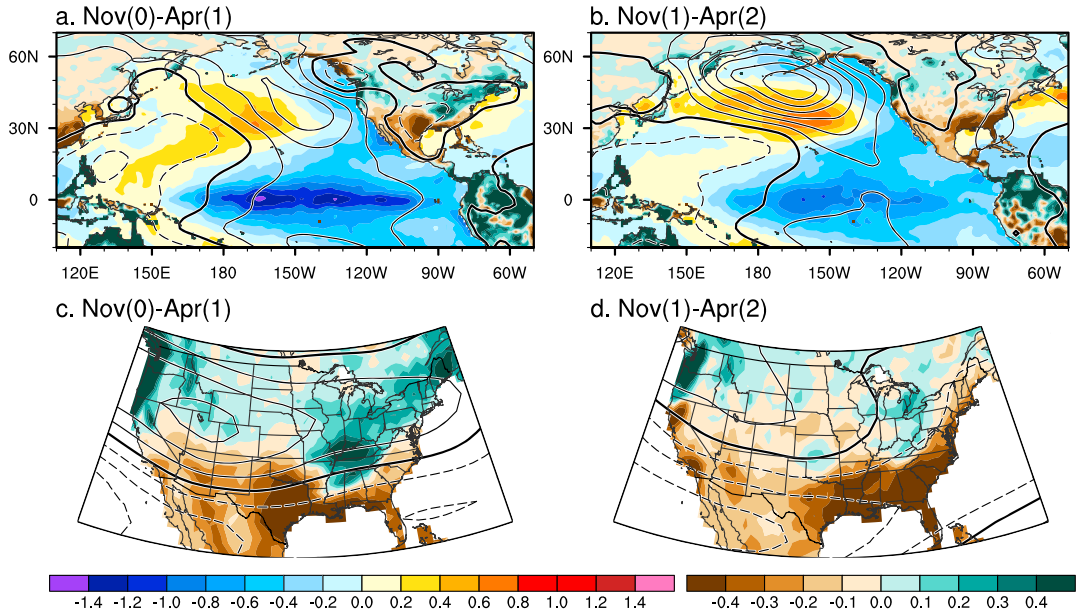

Figure 1. Observed ocean-atmosphere anomaly patterns during the first and second cold seasons of a composite multiyear La Niña event. (a and b) SST (shading over the ocean, °C), terrestrial precipitation (shading over land, mm d^{-1}), and SLP (contours at intervals of 0.5 hPa) anomalies over the Pacific-North American sector and (c and d) terrestrial precipitation (shading over land, mm d^{-1}) and U200 (contours at intervals of 1 m s^{-1}) anomalies over the U.S. for November (0) to April (1) (Figures 1a and 1c) and November (1) to April (2) (Figures 1b and 1d). Based on the HadISST, GPCC, and 20CR data sets for 1901–2012.

season whereas it remains largely unchanged in the off-equatorial region of the tropical Pacific (cf. Figure 2d). The weaker equatorial SST cooling in the second year may be attributed to a slow recharge of the equatorial ocean heat content and resultant weakening of the thermocline feedback (Choi et al., 2013; DiNezio & Deser, 2014; Nagura et al., 2008). Despite the significant weakening of the equatorial cooling, both the North Pacific SLP and SST responses strengthen and show more zonally elongated patterns in the second year compared to the first year. Also, the precipitation reductions over the southern U.S. remain of similar amplitude in the two cold seasons, although they shift eastward and northward, consistent with a northeastward shift of the anomalous easterly winds in the upper troposphere. The eastward shift of the region of reduced precipitation is also associated with a change in sign of the local SLP response. La Niña's impacts on North Pacific SST and SLP and southeastern U.S. precipitation become more statistically significant in the second cold season compared to the first, although the differences between the 2 years are only marginally significant over limited regions (Figures S3 and S4). The fact that these features of the composite analysis described above are robust to choice of data set and sampling of events (Figures S6 and S7) suggests that there are explicit mechanisms underlying them.

What causes the differences in teleconnection patterns between the first and second cold seasons of multiyear La Niña events? As shown in Figure 2, suppressed precipitation and resultant diabatic cooling in the equatorial Pacific induce upper tropospheric cyclonic circulation anomalies on both sides of the equator and emanation of a Rossby wave train into the NH. In the first year, the wave train shows the classical Pacific-North American pattern that arches from the subtropical North Pacific to the southeastern U.S. (Figure 2a). In the second year, however, Z200 anomalies become more zonally elongated and the wave train stretches more toward the pole compared to the first year (Figure 2b). The Z200 anomaly pattern in the second year has some projection onto the northern annular mode (e.g., Thompson & Wallace, 2000) (Figure S8). These changes in the zonal scale and raypath of the Rossby wave response between the first and second years are consistent with linear wave theory (Hoskins & Ambrizzi, 1993), which shows that the raypath radius of curvature of a Rossby wave propagating into the extratropics is proportional to its zonal wavelength. The relative increase in zonal length scale of the Z200 anomalies in the second cold season occurs in conjunction with a relative increase in negative precipitation anomalies over the western tropical Pacific (Figure 2c).

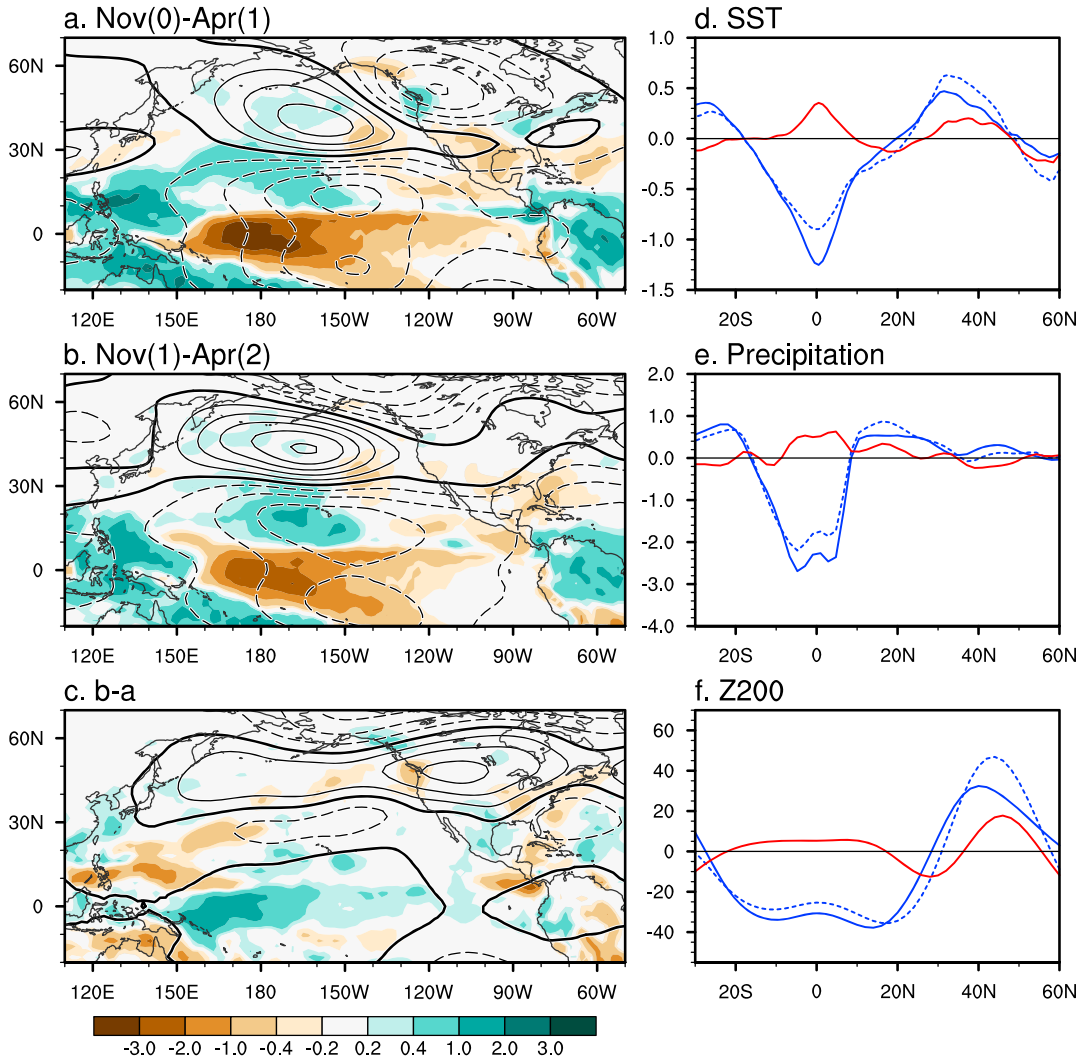

Figure 2. Observed atmospheric anomaly patterns during the first and second cold seasons of a composite multiyear La Niña event. Precipitation (shading, mm d^{-1}) and Z200 (contours at intervals of 10 m) anomalies over the Pacific-North American sector for (a) November (0) to April (1), (b) November (1) to April (2), and (c) their difference (the second minus the first year). Based on the 20CR data set for 1901–2012. Meridional profiles of observed ocean-atmosphere anomalies in the central Pacific (150°W–180°) during the first and second cold seasons of a composite multiyear La Niña event. (d) SST (°C), (e) precipitation (mm d^{-1}), and (f) Z200 anomalies (m) for November (0) to April (1) (blue solid line), November (1) to April (2) (blue dashed line), and their difference (the second minus the first year; red). Based on the HadISST and 20CR data sets for 1901–2012.

The Rossby wave raypath change does not explain why the North Pacific atmospheric circulation response becomes stronger and the subtropical westerly jet shifts farther to the north in the second cold season compared to the first. However, concomitant changes in the meridional profiles of the tropical SST and precipitation responses may help to explain these extratropical changes. The main difference in tropical Pacific SST forcing between the first and second years is the lack of sharp equatorial cooling in the second year (Figure 2d). The relative equatorial warming in the second year is associated with precipitation increase in the deep tropics (Figure 2e) and Z200 anomalies with meridional scales smaller than those in the first year (Figure 2f). These "short wave" Z200 anomalies expand subtropical anomalies to the north and enhance extratropical anomalies in the second year compared to the first, displacing the subtropical westerly jet farther to the north and strengthening the Aleutian low response.

Intriguingly, Z200 differences between the first and second years show a zonally symmetric pattern that extends over the North America sector (Figure 2c). Previous studies of ENSO teleconnections show that in

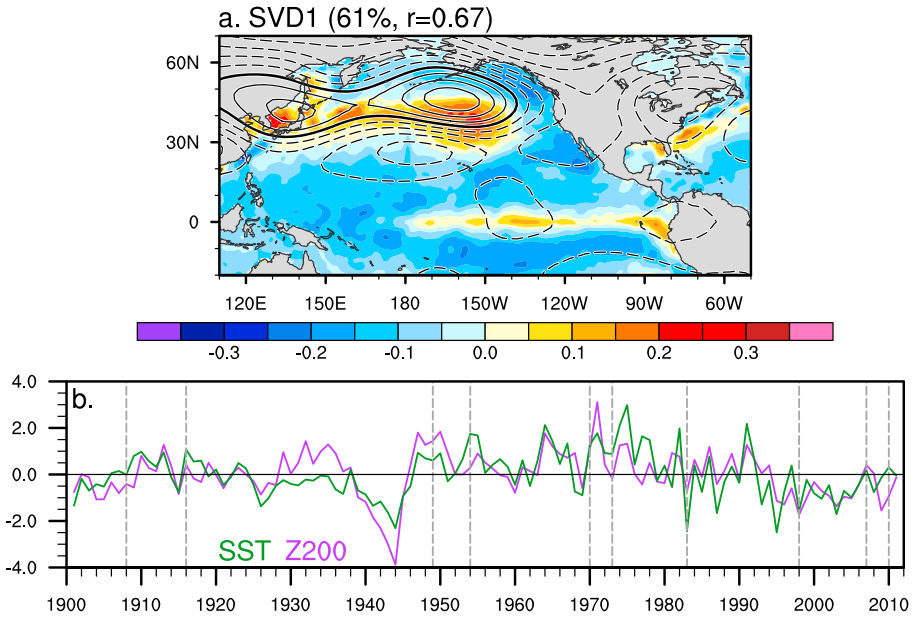

Figure 3. Pattern and time series associated with the first SVD mode of cold season tropical Pacific SST (20°S–20°N, 140°E–80°W) and North Pacific Z200 (10°–70°N, 130°E–70°W) anomalies. Linear regressions on the Niño-3.4 index are removed from both fields prior to the analysis. This mode explains 61% of the total squared covariance. The expansion coefficients are correlated at a coefficient of 0.67. (a) Regression map of SST (shading, °C) and Z200 (contours at intervals of 2.5 m) based on the standardized SST expansion coefficient. (b) Standardized time series of SST (green) and Z200 (purple) expansion coefficients. Year 0 of multiyear La Niña events are indicated by gray dashed lines. Based on the HadISST and 20CR data sets for 1901–2012.

addition to a Rossby wave forced by zonally asymmetric tropical heating, tropical-wide tropospheric temperature changes drive zonally symmetric circulation anomalies in the extratropics via changes in transient eddy momentum fluxes (L'Heureux & Thompson, 2006; Robinson, 2002; Seager et al., 2003). In the second year of multiyear La Niña events, the tropical Atlantic cools significantly while the equatorial Pacific warms compared to the first year (Figure S3c). The resultant weakening of the zonal asymmetry in tropical SST forcing may increase the relative importance of eddy-driven teleconnections although this mechanism does not explain the change in meridional scale of the teleconnections. Significant changes are also found in precipitation over the tropical Indian Ocean between the first and second years of multiyear La Niña events (Figure S3l), which may affect the North Pacific atmospheric circulation as suggested by previous studies (e.g., Alexander et al., 2002; Annamalai et al., 2007; Spencer et al., 2004). These changes in meridional and zonal structure of the teleconnections are evident for different data sets and analysis periods (not shown).

Whereas the changes in teleconnection patterns between the first and second cold seasons of multiyear La Niña events are robust in the observational composite analysis (Figures S6 and S7), atmospheric general circulation models forced with observed SSTs have difficulty reproducing the observed changes (Figures S7 and S9–S11). Extratropical atmospheric circulation anomalies show zonally elongated patterns in both the first and second cold seasons in all the simulations, and the Aleutian low response weakens in the second year in all but the AM2.1 simulation (Figures S7 and S9). U.S. precipitation anomalies also show similar patterns between the first and second years, and the northeastward expansion of negative anomalies in the second year is not reproduced except in CAM4 (Figure S9). Compared to observations, tropical Pacific precipitation anomalies simulated in the CAM are confined more to the deep tropics in both years, and the difference in precipitation response between the first and second years shows meridional scales similar to those for the first and second years (Figures S10 and S11). The AM2.1 and one of the CAM5 experiments simulate the observed change in the meridional scale of tropical precipitation anomalies, but only the AM2.1 reproduces the zonally symmetric response to equatorial warming in the second year similar to observations. Further studies are needed to better understand the mechanisms of multiyear La Niña teleconnections and the causes of model deficiencies. The strong zonal symmetry in both the first and second years of multiyear La Niña events in CAM and AM2.1 suggests that eddy-driven teleconnections may be too strong in these models.

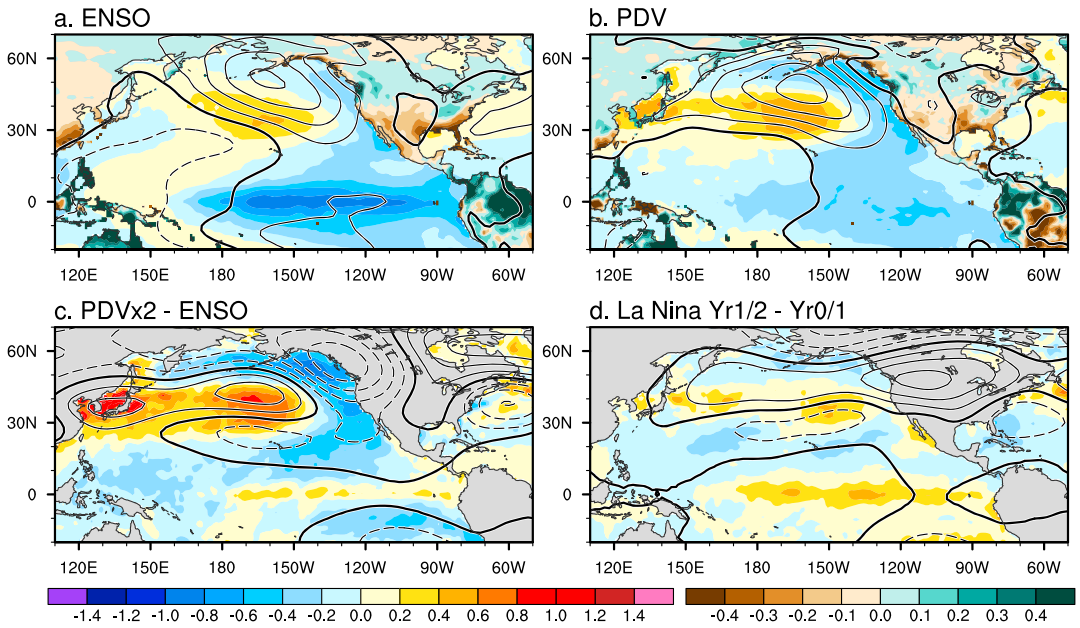

Figure 4. Observed ocean-atmosphere anomaly patterns during the cold season for (a) the ENSO and (b) PDV. November–April SST (shading over the ocean, °C), terrestrial precipitation (shading over land, mm d^{-1}), and SLP (contours at intervals of 0.5 hPa) anomalies over the Pacific-North American sector. The ENSO pattern is based on linear regressions on the standardized Niño-3.4 index. The PDV pattern is obtained by taking differences between the positive and negative phases of PDV ((1925–1946, 1977–1997) minus (1901–1924, 1947–1976, 1998–2012)) based on Newman et al. (2016). The sign is reversed in both the ENSO and PDV maps for a comparison with Figure 1. Differences of observed ocean-atmosphere anomaly patterns during the cold season between (c) the ENSO and PDV and (d) the first and second years of a composite multiyear La Niña event (the second minus the first year). November–April SST (shading, °C) and Z200 (contours at intervals of 10 m) anomalies over the Pacific-North American sector. In Figure 4c, the PDV pattern is multiplied by a factor of 2 before taking differences with the ENSO pattern to better represent a change in the meridional structure of tropical SST anomalies. Based on the HadISST, GPCC, and 20CR data sets for 1901–2012.

Based on the comparison of observed teleconnection patterns between the first and second cold seasons of multiyear La Niña events, we postulate that the large-scale atmospheric circulation is more sensitive to broad tropical SST anomalies than those intensified at the equator. To further understand how the spatial structure of tropical SST forcing influences NH teleconnections, we conduct a singular value decomposition (SVD) analysis (Bretherton et al., 1992) of cold season tropical Pacific SST (20°S–20°N, 140°E–80°W) and North Pacific Z200 (10°–70°N, 130°E–70°W) anomalies (Figure 3). Prior to the SVD analysis, we remove the component linearly related to the Niño-3.4 index from both the SST and Z200 fields via regression analysis to highlight the deviations from average ENSO pattern. The first SVD mode, which explains 61% of the total squared covariance, clearly indicates a linkage between the equatorial intensification of tropical Pacific SST anomalies and a zonally symmetric pattern of Z200 anomalies that has a meridional scale smaller than typical ENSO teleconnections (cf. Figure 2a). This mode shows that weaker amplitude SST cooling along the equator relative to the subtropics (i.e., warming along the equator relative to off the equator) is associated with a decrease in Z200 in the subtropics and an increase in midlatitudes across the Pacific basin, consistent with the composite analysis of multiyear La Niña teleconnections (Figure 4d). Similar Z200 and SST patterns appear as the first and second leading empirical orthogonal function modes of their individual fields, respectively (not shown). The equatorward SST gradient associated with the SVD mode is also accompanied by precipitation increase in the central equatorial Pacific and decrease over the Indo-Pacific warm pool (Figure S12) as in the composite analysis of multiyear La Niña (Figures 2c and S3l). The SST and Z200 expansion coefficients of this SVD mode are correlated at a coefficient of 0.67, and both increase from the first to the second year of a composite multiyear La Niña event although there are large variations among events (Figure 3b).

The SST and Z200 expansion coefficients of the first SVD mode exhibit distinct interdecadal variability with predominantly negative phases from the mid-1920s to the mid-1940s and after the early 1980s and a

positive phase between them (Figure 3b), roughly corresponding to the known phases of Pacific decadal variability (PDV) (e.g., Chen & Wallace, 2015; Deser et al., 2004; Garreaud & Battisti, 1999; Newman et al., 2016). As discussed by many previous studies, PDV shows a broader meridional structure of tropical Pacific SST anomalies than ENSO due to the absence of a narrow equatorial maximum. Figures 4a and 4b compare the observed ENSO and PDV anomaly patterns of SST, SLP, and terrestrial precipitation for the NH cold season. Despite much weaker equatorial SST anomalies, North Pacific SLP and SST anomalies are large and more zonally elongated for PDV compared to ENSO, similar to Figures 1a and 1b for multiyear La Niña events. The differences in SST and Z200 anomaly patterns between the ENSO and PDV (Figure 4c) are also similar to the differences between the first and second years of multiyear La Niña events (Figure 4d) and to the leading SVD pattern (Figure 3a) over the North Pacific, although the zonal symmetry of Z200 anomalies is less pronounced in the PDV-ENSO and SVD patterns. Thus, the mechanisms that modulate the teleconnection patterns between the first and second cold seasons of multiyear La Niña events may also explain the differences between the ENSO and PDV anomaly patterns. In support of this notion, the result of SVD analysis is insensitive to temporal filtering of the data (not shown). It should be noted, however, that the causality of tropical and extratropical anomalies for PDV remains subject to debate (e.g., Liu, 2012; Newman et al., 2016; Okumura, 2013). Unlike ENSO, in which extratropical ocean-atmosphere anomalies are primarily driven by tropical SSTs, stochastic atmospheric forcing in the extratropics may play a more important role for PDV. Our result nonetheless suggests that the larger relative amplitude of extratropical ocean-atmosphere anomalies does not necessarily indicate a lesser role of tropical SST forcing.

4. Summary and Discussion

Based on a composite analysis of observational and reanalysis data, we show that multiyear La Niña events exert significant impacts on the atmospheric circulation and drought conditions over the southern U.S. during the NH cold season. Although the equatorial Pacific SST cooling weakens significantly from the first to the second year, La Niña teleconnections do not weaken proportionally. Compared to the first year, extratropical atmospheric circulation anomalies show a more zonally elongated pattern and become even larger over the North Pacific in the second year. Over the U.S., precipitation anomalies have similar magnitude in both years and the region of reduced precipitation expands to the north and shifts eastward in the second year compared to the first year in association with the farther northward displacement of the subtropical westerly jet. These modulations of teleconnection patterns in the second year appear to be related to changes in the zonal and meridional structures of tropical precipitation anomalies. While the increased zonal extent of tropical precipitation and circulation anomalies may increase the raypath radius of curvature of the Rossby wave response, the reduced equatorial precipitation anomalies associated with the weaker SST cooling seem to shift the subtropical westerly jet farther to the north and enhance the Aleutian low response. We speculate that the same mechanism may also apply to the differences between the ENSO and PDV patterns.

Given the extended impacts on droughts, it is important to be able to predict the duration of La Niña events. An early warning of multiyear La Niña would allow us to take cautionary actions on water conservation and agricultural planning. The current operational ENSO forecasts are, however, limited to 8 months (Barnston et al., 2012), precluding the predictions of multiyear La Niña events. Through idealized model experiments, DiNezio, Deser, Okumura, et al. (2017) show that multiyear La Niña events can be predicted before the initial onset when they are preceded by strong El Niño events and associated large discharge of the equatorial ocean heat content. It is interesting to note that multiyear La Niña events became more frequent after the 1970s along with an increase in ENSO amplitude (Figure S1), consistent with an analysis of a long climate model simulation (Okumura et al., 2017). Further studies are needed to demonstrate the feasibility of operational predictions of La Niña duration (DiNezio, Deser, Karspeck, et al., 2017), as well as to understand the processes affecting the duration of individual La Niña events.

For successful predictions of droughts driven by multiyear La Niña, we also need to address the uncertainty of atmospheric teleconnections (e.g., Deser et al., 2017; Schubert et al., 2016; Seager & Hoerling, 2014). Although the composite multiyear La Niña teleconnection patterns are robust across different data sets and sampling of events, individual events may deviate from this composite picture. For example, during the most recent multiyear La Niña event of 2010–2012, the Aleutian low response weakened and precipitation increased over the southeastern U.S. in the second cold season (Fernando et al., 2016). The event-to-event variations in

teleconnections are likely to arise from both predictable and unpredictable factors. For the predictable component, variations in the pattern and magnitude of SST anomalies are likely to cause different teleconnections, which can be potentially simulated by atmospheric models with a large number of ensemble members. In any single member of atmospheric model simulations, as well as in reality, the predictable component can be obscured by internal variability of the atmosphere, which is unpredictable even with a perfect model. A more systematic and quantitative assessment is necessary to understand the predictability of La Niña teleconnections. We will also need to reevaluate the atmospheric models used for seasonal climate forecasts for their ability to simulate the evolution of multiyear La Niña teleconnections.

Multiyear La Niña events have significant impacts on precipitation over the southern U.S. mostly during the NH cold season. It remains to be examined how the precipitation deficit in cold season affects the onset and evolution of drought over the southern U.S. during the intervening seasons. For example, Anderson et al. (2016) shows that ENSO-induced wintertime precipitation anomalies affect soil moisture and crop yield over the southern Great Plain states in the following seasons. In addition to the soil moisture memory, positive land-atmosphere feedback may also play an important role in perpetuating the drought (e.g., Hong & Kalnay, 2000; Koster et al., 2004; Lyon & Dole, 1995; Oglesby & Erickson, 1989; Schubert et al., 2004; Trenberth & Branstator, 1992). The drier soil after the first peak of La Niña is likely to increase surface air temperatures by decreasing available moisture for evaporation and resultant latent heat loss. The increased air temperatures would, in turn, enhance evaporation from the surface, further drying the soil. The return of La Niña and associated dry winter conditions in the second year may thus have more severe impacts on the regional hydrological cycle and ecosystem than in the first year. Further understanding of the mechanisms and predictability of multiyear La Niña events and their impacts is critical to minimize the calamity of persistent droughts over the southern U.S.

Acknowledgments

The authors would like to thank John M. Wallace and Weston Anderson for helpful discussions and two anonymous reviewers for their insightful comments and constructive suggestions. The observational data sets used in this study are obtained online: HadISST from the Met Office Hadley Center (http://www.metoffice.gov.uk/hadobs/); GPCC, 20CR, NCEP-NCAR, and OISST from the NOAA Earth System Research Laboratory Physical Science Division (https://www.esrl.noaa.gov/psd/); and ERA-Interim from the ECMWF (http://www.ecmwf.int/). The CAM simulations are available through the Climate Variability and Change Working Group of the Climate Earth System Model (http://www.cesm.ucar.edu/working_groups/CVC/). The GFDL AM2.1 simulation is provided by courtesy of Jian Lu and Fanrong Zeng. This study is supported by the NOAA Climate Program Office Modeling, Analysis, Predictions, and Projections Program (NA14OAR4310227, NA14OAR4310228, NA14OAR4310229, NA17OAR4310149, and NA17OAR4310145). NCAR is sponsored by the National Science Foundation.

References

Alexander, M. A., Bladé, I., Newman, M., Lanzante, J. R., Lau, N.-C., & Scott, J. D. (2002). The atmospheric bridge: The influence of ENSO teleconnections on air–sea interaction over the global oceans. *Journal of Climate*, *15*(16), 2205–2231. https://doi.org/10.1175/1520-0442(2002)015%3C2205:TABTIO%3E2.0.CO;2

Anderson, W., Seager, R., Baethgen, W., & Cane, M. (2016). Life cycles of agriculturally relevant ENSO teleconnections in North and South America. *International Journal of Climatology*, *15*(16), 2205. https://doi.org/10.1016/j.agsy.2014.01.002

Annamalai, H., Okajima, H., & Watanabe, M. (2007). Possible impact of the Indian Ocean SST on the Northern Hemisphere circulation during El Niño. *Journal of Climate*, *20*(13), 3164–3189. https://doi.org/10.1175/JCLI4156.1

Barnston, A. G., Tippett, M. K., L'Heureux, M. L., Li, S., & DeWitt, D. G. (2012). Skill of real-time seasonal ENSO model predictions during 2002–11: Is our capability increasing? *Bulletin of the American Meteorological Society*, *93*(5), 631–651. https://doi.org/10.1175/BAMS-D-11-00111.1

Bretherton, C. S., Smith, C., & Wallace, J. M. (1992). An intercomparison of methods for finding coupled patterns in climate data. *Journal of Climate*, *5*(6), 541–560. https://doi.org/10.1175/1520-0442(1992)005%3C0541:AIOMFF%3E2.0.CO;2

Burgers, G., & Stephenson, D. B. (1999). The "normality" of El Niño. *Geophysical Research Letters*, *26*(8), 1027–1030. https://doi.org/10.1029/1999GL900161

Chang, P., Yamagata, T., Schopf, P., Behera, S. K., Carton, J., Kessler, W. S., … Xie, S.-P. (2006). Climate fluctuations of tropical coupled systems-the role of ocean dynamics. *Journal of Climate*, *19*(20), 5122–5174. https://doi.org/10.1175/JCLI3903.1

Chen, X., & Wallace, J. M. (2015). ENSO-like variability: 1900–2013. *Journal of Climate*, *28*(24), 9623–9641. https://doi.org/10.1175/JCLI-D-15-0322.1

Choi, K. Y., Vecchi, G. A., & Wittenberg, A. T. (2013). ENSO transition, duration, and amplitude asymmetries: Role of the nonlinear wind stress coupling in a conceptual model. *Journal of Climate*, *26*(23), 9462–9476. https://doi.org/10.1175/JCLI-D-13-00045.1

Cole, J. E., Overpeck, J. T., & Cook, E. R. (2002). Multiyear La Niña events and persistent drought in the contiguous United States. *Geophysical Research Letters*, *29*(13), 1647. https://doi.org/10.1029/2001GL013561

Compo, G. P., Whitaker, J. S., Sardeshmukh, P. D., Matsui, N., Allan, R. J., Yin, X., … Worley, S. J. (2011). The twentieth century reanalysis project. *Quarterly Journal of the Royal Meteorological Society*, *137*(654), 1–28. https://doi.org/10.1002/qj.776

Dai, A., Trenberth, K. E., & Karl, T. R. (1998). Global variations in droughts and wet spells: 1900–1995. *Geophysical Research Letters*, *25*(17), 3367–3370. https://doi.org/10.1029/98GL52511

Dee, D. P., Uppala, S., Simmons, A., Berrisford, P., Poli, P., Kobayashi, S., … Vitart, F. (2011). The ERA-Interim reanalysis: Configuration and performance of the data assimilation system. *Quarterly Journal of the Royal Meteorological Society*, *137*(656), 553–597. https://doi.org/10.1002/qj.828

Deser, C., Phillips, A. S., & Hurrell, J. W. (2004). Pacific interdecadal climate variability: Linkages between the tropics and the North Pacific during boreal winter since 1900. *Journal of Climate*, *17*(16), 3109–3124. https://doi.org/10.1175/1520-0442(2004)017%3C3109:PICVLB%3E2.0.CO;2

Deser, C., Simpson, I. R., McKinnon, K. A., & Phillips, A. S. (2017). The Northern Hemisphere extratropical atmospheric circulation response to ENSO: How well do we know it and how do we evaluate models accordingly? *Journal of Climate*. https://doi.org/10.1175/JCLI-D-16-0844.1

DiNezio, P. N., & Deser, C. (2014). Nonlinear controls on the persistence of La Niña. *Journal of Climate*, *27*(19), 7335–7355. https://doi.org/10.1175/JCLI-D-14-00033.1

DiNezio, P. N., Deser, C., Karspeck, A., Yeager, S., Okumura, Y., Danabasoglu, G., … Meehl, G. A. (2017). A two-year forecast for a 60–80% chance of La Niña in 2017–18, *Geophysical Research Letters*, *44*, https://doi.org/10.1002/2017GL074904

DiNezio, P. N., Deser, C., Okumura, Y., & Karspeck, A. (2017). Predictability of 2-year La Niña events in a coupled general circulation model. *Climate Dynamics*. https://doi.org/10.1007/s00382-017-3575-3

Dommenget, D., Bayr, T., & Frauen, C. (2013). Analysis of the non-linearity in the pattern and time evolution of El Niño southern oscillation. *Climate Dynamics*, *40*(11-12), 2825–2847. https://doi.org/10.1007/s00382-012-1475-0

Fernando, D. N., Mo, K. C., Fu, R., Pu, B., Bowerman, A., Scanlon, B. R., … Zhang, K. (2016). What caused the spring intensification and winter demise of the 2011 drought over Texas? *Climate Dynamics*, *47*(9-10), 3077–3090. https://doi.org/10.1007/s00382-016-3014-x

Garreaud, R., & Battisti, D. S. (1999). Interannual (ENSO) and interdecadal (ENSO-like) variability in the Southern Hemisphere tropospheric circulation. *Journal of Climate*, *12*(7), 2113–2123. https://doi.org/10.1175/1520-0442(1999)012%3C2113:IEAIEL%3E2.0.CO;2

Hoerling, M., & Kumar, A. (2003). The perfect ocean for drought. *Science*, *299*(5607), 691–694. https://doi.org/10.1126/science.1079053

Hoerling, M. P., Kumar, A., & Zhong, M. (1997). El Niño, La Niña, and the nonlinearity of their teleconnections. *Journal of Climate*, *10*(8), 1769–1786. https://doi.org/10.1175/1520-0442(1997)010%3C1769:ENOLNA%3E2.0.CO;2

Hong, S.-Y., & Kalnay, E. (2000). Role of sea surface temperature and soil-moisture feedback in the 1998 Oklahoma-Texas drought. *Nature*, *408*(6814), 842–844. https://doi.org/10.1038/35048548

Hoskins, B. J., & Ambrizzi, T. (1993). Rossby wave propagation on a realistic longitudinally varying flow. *Journal of the Atmospheric Sciences*, *50*(12), 1661–1671. https://doi.org/10.1175/1520-0469(1993)050%3C1661:RWPOAR%3E2.0.CO;2

Hu, Z.-Z., Kumar, A., Xue, Y., & Jha, B. (2014). Why were some La Niñas followed by another La Niña? *Climate Dynamics*, *42*(3-4), 1029–1042. https://doi.org/10.1007/s00382-013-1917-3

Huang, B., Banzon, V. F., Freeman, E., Lawrimore, J., Liu, W., Peterson, T. C., … Zhang, H.-M. (2015). Extended Reconstructed Sea Surface Temperature version 4 (ERSST.v4). Part I: Upgrades and intercomparisons. *Journal of Climate*, *28*(3), 911–930. https://doi.org/10.1175/JCLI-D-14-00006.1

Hurrell, J. W., Hack, J. J., Shea, D., Caron, J. M., & Rosinski, J. (2008). A new sea surface temperature and sea ice boundary dataset for the Community Atmosphere Model. *Journal of Climate*, *21*(19), 5145–5153. https://doi.org/10.1175/2008JCLI2292.1

Hurrell, J. W., Holland, M. M., Gent, P. R., Ghan, S., Kay, J. E., Kushner, P. J., … Marshall, S. (2013). The Community Earth System Model: A framework for collaborative research. *Bulletin of the American Meteorological Society*, *94*(9), 1339–1360. https://doi.org/10.1175/BAMS-D-12-00121.1

Kalnay, E., Kanamitsu, M., Kistler, R., Collins, W., Deaven, D., Gandin, L., … Joseph, D. (1996). The NCEP/NCAR 40-year reanalysis project. *Bulletin of the American Meteorological Society*, *77*(3), 437–471. https://doi.org/10.1175/1520-0477(1996)077%3C0437:TNYRP%3E2.0.CO;2

Kang, I.-S., & Kug, J. S. (2002). El Niño and La Niña sea surface temperature anomalies: Asymmetry characteristics associated with their wind stress anomalies, *Journal of Geophysical Research*, *107*(D19), 4372. https://doi.org/10.1029/2001JD000393.

Kessler, W. S. (2002). Is ENSO a cycle or a series of events? *Geophysical Research Letters*, *29*(23), 2125. https://doi.org/10.1029/2002GL015924

Kiladis, G. N., & Diaz, H. F. (1989). Global climatic anomalies associated with extremes in the Southern Oscillation. *Journal of Climate*, *2*(9), 1069–1090. https://doi.org/10.1175/1520-0442(1989)002%3C1069:GCAAWE%3E2.0.CO;2

Koster, R. D., Dirmeyer, P. A., Guo, Z., Bonan, G., Chan, E., Cox, P., … GLACE Team (2004). Regions of strong coupling between soil moisture and precipitation. *Science*, *305*(5687), 1138–1140. https://doi.org/10.1126/science.1100217

Lau, K. M., & Sheu, P. J. (1988). Annual cycle, quasi-biennial oscillation, and southern oscillation in global precipitation. *Journal of Geophysical Research*, *93*(D9), 10,975–10,988. https://doi.org/10.1029/JD093iD09p10975

L'Heureux, M. L., & Thompson, D. (2006). Observed relationships between the El Niño–Southern Oscillation and the extratropical zonal-mean circulation. *Journal of Climate*, *19*(2), 276–287. https://doi.org/10.1175/JCLI3617.1

Li, H., Dai, A., Zhou, T., & Lu, J. (2010). Responses of East Asian summer monsoon to historical SST and atmospheric forcing during 1950–2000. *Climate Dynamics*, *34*(4), 501–514.

Liu, Z. (2012). Dynamics of interdecadal climate variability: A historical perspective. *Journal of Climate*, *25*(6), 1963–1995. https://doi.org/10.1175/2011JCLI3980.1

Lyon, B., & Dole, R. M. (1995). A diagnostic comparison of the 1980 and 1988 U.S. summer heat wave-droughts. *Journal of Climate*, *8*(6), 1658–1675. https://doi.org/10.1175/1520-0442(1995)008%3C1658:ADCOTA%3E2.0.CO;2

McGregor, S., Ramesh, N., Spence, P., England, M. H., McPhaden, M. J., & Santoso, A. (2013). Meridional movement of wind anomalies during ENSO events and their role in event termination. *Geophysical Research Letters*, *40*, 749–754. https://doi.org/10.1002/grl.50136

McPhaden, M. J., & Zhang, X. (2009). Asymmetry in zonal phase propagation of ENSO sea surface temperature anomalies. *Geophysical Research Letters*, *36*, L13703. https://doi.org/10.1029/2009GL038774

Mo, K. C., & Schemm, J. E. (2008). Relationships between ENSO and drought over the southeastern United States. *Geophysical Research Letters*, *35*, L15701. https://doi.org/10.1029/2008GL034656

Nagura, M., Ando, K., & Mizuno, K. (2008). Pausing of the ENSO cycle: A case study from 1998 to 2002. *Journal of Climate*, *21*(2), 342–363. https://doi.org/10.1175/2007JCLI1765.1

Neelin, J. D., Battisti, D. S., Hirst, A. C., Jin, F. F., Wakata, Y., Yamagata, T., & Zebiak, S. E. (1998). ENSO theory. *Journal of Geophysical Research*, *103*(C7), 14,261–14,290. https://doi.org/10.1029/97JC03424

Newman, M., Alexander, M. A., Ault, T. R., Cobb, K. M., Deser, C., Di Lorenzo, E., … Smith, C. A. (2016). The Pacific decadal oscillation, revisited. *Journal of Climate*, *29*(12), 4399–4427. https://doi.org/10.1175/JCLI-D-15-0508.1

Oglesby, R. J., & Erickson, D. J. III (1989). Soil moisture and the persistence of North American drought. *Journal of Climate*, *2*(11), 1362–1380. https://doi.org/10.1175/1520-0442(1989)002%3C1362:SMATPO%3E2.0.CO;2

Ohba, M., & Ueda, H. (2009). Role of nonlinear atmospheric response to SST on the asymmetric transition process of ENSO. *Journal of Climate*, *22*(1), 177–192. https://doi.org/10.1175/2008JCLI2334.1

Okumura, Y. M. (2013). Origins of tropical Pacific decadal variability: Role of stochastic atmospheric forcing from the South Pacific. *Journal of Climate*, *26*(24), 9791–9796. https://doi.org/10.1175/JCLI-D-13-00448.1

Okumura, Y. M., & Deser, C. (2010). Asymmetry in the duration of El Niño and La Niña. *Journal of Climate*, *23*(21), 5826–5843. https://doi.org/10.1175/2010JCLI3592.1

Okumura, Y. M., Sun, T., & Wu, X. (2017). Asymmetric modulation of El Niño and La Niña and the linkage to tropical Pacific decadal variability. *Journal of Climate*, *30*(12), 4705–4733. https://doi.org/10.1175/JCLI-D-16-0680.1

Rayner, N. A., Parker, D. E., Horton, E. B., Folland, C. K., Alexasnder, L. V., Rowell, D. P., … Kaplan, A. (2003). Global analyses of sea surface temperature, sea ice, and night marine air temperature since the late nineteenth century, *Journal of Geophysical Research*, *108*(D14), 4407. https://doi.org/10.1029/2002JD002670.

Reynolds, R. W., Rayner, N. A., Smith, T. M., Stokes, D. C., & Wang, W. (2002). An improved in situ and satellite SST analysis for climate. *Journal of Climate*, *15*(13), 1609–1625. https://doi.org/10.1175/1520-0442(2002)015%3C1609:AIISAS%3E2.0.CO;2

Robinson, W. A. (2002). On the midlatitude thermal response to tropical warmth, *Geophysical Research Letters*, *29*(8), 1190. https://doi.org/10.1029/2001GL014158

Ropelewski, C. F., & Halpert, M. S. (1989). Precipitation patterns associated with the high index phase of the Southern Oscillation. *Journal of Climate*, *2*(3), 268–284. https://doi.org/10.1175/1520-0442(1989)002%3C0268:PPAWTH%3E2.0.CO;2

Schneider, U., Ziese, M., Meyer-Christoffer, A., Finger, P., Rustemeier, E., & Becker, A. (2016). The new portfolio of global precipitation data products of the global precipitation climatology centre suitable to assess and quantify the global water cycle and resources, proceedings of the international association of hydrological. *Sciences*, *374*, 29–34.

Schubert, S. D., Stewart, R. E., Wang, H., Barlow, M., Berbery, E. H., Cai, W., … Zhou, T. (2016). Global meteorological drought: A synthesis of current understanding with a focus on SST drivers of precipitation deficits. *Journal of Climate*, *29*(11), 3989–4019. https://doi.org/10.1175/JCLI-D-15-0452.1

Schubert, S. D., Suarez, M. J., Pegion, P. J., Koster, R. D., & Bacmeister, J. T. (2004). Causes of long-term drought in the U.S. Great Plains. *Journal of Climate*, *17*(3), 485–503. https://doi.org/10.1175/1520-0442(2004)017%3C0485:COLDIT%3E2.0.CO;2

Seager, R., Harnik, N., Kushnir, Y., Robinson, W., & Miller, J. (2003). Mechanisms of hemispherically symmetric climate variability. *Journal of Climate*, *16*(18), 2960–2978. https://doi.org/10.1175/1520-0442(2003)016%3C2960:MOHSCV%3E2.0.CO;2

Seager, R., Harnik, N., Robinson, W. A., Kushnir, Y., Ting, M., Huang, H.-P., & Velez, J. (2005). Mechanisms of ENSO-forcing of hemispherically symmetric precipitation variability. *Quarterly Journal of the Royal Meteorological Society*, *131*(608), 1501–1527. https://doi.org/10.1256/qj.04.96

Seager, R., & Hoerling, M. (2014). Atmosphere and ocean origins of North American droughts. *Journal of Climate*, *27*(12), 4581–4606. https://doi.org/10.1175/JCLI-D-13-00329.1

Seager, R., Kushnir, Y., Herweijer, C., Naik, N., & Velez, J. (2005). Modeling of tropical forcing of persistent droughts and pluvials over western North America: 1856-2000. *Journal of Climate*, *18*(19), 4065–4088. https://doi.org/10.1175/JCLI3522.1

Spencer, H., Slingo, J. M., & Davey, M. K. (2004). Seasonal predictability of ENSO teleconnections: The role of the remote ocean response. *Climate Dynamics*, *22*(5), 511–526. https://doi.org/10.1007/s00382-004-0393-1

Thompson, D. W., & Wallace, J. M. (2000). Annular modes in the extratropical circulation. Part I: Month-to-month variability. *Journal of Climate*, *13*(5), 1000–1016. https://doi.org/10.1175/1520-0442(2000)013%3C1000:AMITEC%3E2.0.CO;2

Trenberth, K. E., & Branstator, G. W. (1992). Issues in establishing causes of the 1988 drought over North America. *Journal of Climate*, *5*(2), 159–172. https://doi.org/10.1175/1520-0442(1992)005%3C0159:IIECOT%3E2.0.CO;2

Trenberth, K. E., Branstator, G. W., Karoly, D., Kumar, A., Lau, N.-C., & Ropelewski, C. (1998). Progress during TOGA in understanding and modeling global teleconnections associated with tropical sea surface temperatures. *Journal of Geophysical Research*, *103*(C7), 14,291–14,324. https://doi.org/10.1029/97JC01444

Wallace, J. M., Rasmusson, E. M., Mitchell, T. P., Kousky, V. E., Sarachik, E. S., & von Storch, H. (1998). On the structure and evolution of ENSO-related climate variability in the tropical Pacific: Lessons from TOGA. *Journal of Geophysical Research*, *103*(C7), 14,241–14,259. https://doi.org/10.1029/97JC02905

Wang, C., & Picaut, J. (2004). *Understanding ENSO physics—A review, Earth's climate: The ocean–atmosphere interaction*, *Geophysical Monograph Series*, (Vol. 147, pp. 21–48). Washington, DC: American Geophysical Union.

Wang, H., & Schubert, S. (2014). The precipitation response over the continental United States to cold tropical Pacific sea surface temperatures. *Journal of Climate*, *27*(13), 5036–5055. https://doi.org/10.1175/JCLI-D-13-00453.1